

**MULTIPLE HYPOTHESIS TRACKING (MHT)  
FOR SPACE SURVEILLANCE:  
RESULTS AND SIMULATION STUDIES**

**Navraj Singh, Joshua T. Horwood, Jeffrey M. Aristoff, and Aubrey B. Poore**

*Numerica Corporation, 4850 Hahns Peak Drive, Suite 200, Loveland CO, 80538*

**Carolyn Sheaff**

*AFRL/RIED, 525 Brooks Road, Rome, NY, 13441*

**Moriba K. Jah**

*AFRL/RVSV, 3550 Aberdeen Avenue SE, Kirtland AFB, NM, 87117*

**ABSTRACT**

The need to accurately track breakups and satellite clusters, as well as to resolve uncorrelated tracks (UCTs), especially uncorrelated optical observations (UCOs), requires new, robust, and autonomous methods for space surveillance to enable the development and maintenance of the space catalog and to support the overall SSA mission. This paper presents results on the performance of a newly-developed, statistically-robust, system-level, multiple hypothesis tracking (MHT) capability for joint catalog maintenance, UCT/UCO resolution, and initial orbit determination, in multiple regimes of space. A recent companion paper described some of the unique components contained within the authors' implementation of MHT, including the multi-frame data association problem and the statistical framework used for scoring the likelihood that a sequence of measurements, UCTs/UCOs, and other reports emanate from a common object (either newly-discovered or already catalogued). As demonstrated by the results in this paper, the MHT system provides superior tracking performance (compared to existing methods for data association) in realistic multi-sensor multi-object tracking scenarios over multiple regimes of space. Specifically, we demonstrate that the prototype MHT system can accurately and efficiently process tens of thousands of UCTs/UCOs emanating from thousands of space objects in realtime on a single processor.

**1. INTRODUCTION**

The Joint Space Operations Center (JSpOC) currently tracks more than 22,000 satellites and space debris orbiting the Earth [1, 2]. With the anticipated installation of more accurate sensors and the increased probability of future collisions between space objects, the potential number of newly-discovered space objects is expected to increase further by an order of magnitude or more within the next decade, thereby placing an ever-increasing burden on current operational systems. Moreover, there is a need to track closely-spaced objects due, for example, to breakups as illustrated by the recent Fengyun 1C breakup and the Iridium-Kosmos collision. It is critical that these new objects, initially declared as uncorrelated tracks (UCTs), be correlated to existing catalogued objects as soon as possible or declared as bona fide new objects. Indeed, one cannot perform conjunction assessment screening until all new debris objects are catalogued or UCTs are resolved. At present, this cataloguing process has been manpower intensive; it can take several months to establish orbits from large breakup events, such as the Fengyun breakup. Moreover, uncorrelated optical observations (UCOs) from electro-optical (EO) sensors are often discarded by existing systems; current methods cannot reliably associate/correlate and fuse multiple UCOs in order to initiate new orbits. Thus, an autonomous realtime capability is needed for breakup and UCT/UCO processing, in all regimes of space, to support more timely and effective conjunction assessment screening on newly discovered debris objects, as well as to support other downstream space situational awareness (SSA) functions.

In order to address some of the future needs of the space surveillance operational system, the authors and their collaborators have developed a new capability that jointly performs catalog maintenance, object identification, UCT/UCO resolution, and initiates orbits on new objects, as needed. A high level of performance is achieved by delaying ambiguous association decisions in contentious regimes especially when

tracking closely-spaced objects and breakups. The underlying algorithm, called *multiple hypothesis tracking (MHT)*, provides a newly-developed, statistically-robust, multi-sensor, system-level (as opposed to sensor-level) tracking solution for both widely- and closely-spaced objects using advanced data association methods, information fusion, and astrodynamics algorithms. This automated MHT system allows for more throughput and lower computational burden on existing systems, while substantially reducing the number of unresolved UCTs/UCOs and enabling more timely cataloging of breakups and debris objects.

In the companion paper [3], we reported on the salient features of the authors’ MHT for space surveillance and the differentiators that set it apart from other tracking and data association methods proposed in the community and from those used in operation. At a high level, the reported technology solves a number of tracking problems *jointly* including space catalog maintenance, UCT/UCO resolution, and cataloging of new breakup objects and other “hard to identify” objects such as high area-to-mass ratio (HAMR) objects in GEO. The strength of MHT lies in its ability to process multiple frames of data *simultaneously* (e.g., data over multiple sensor looks) which provides the ability to hold difficult association decisions in abeyance until more information (data) becomes available\*. This multi-frame processing feature is essential for tracking *closely-spaced objects*; though MHT can adapt to single-frame processing or even a hypothesis-less method when the association is unambiguous. Moreover, the MHT framework incorporates multiple hypotheses for report-to-system-track data association and uses a multi-arc construction to accommodate recently developed algorithms for multiple hypothesis filtering (e.g., AEGIS [4], CAR-MHF [5], and MMAE [6]).

The underlying data association problem of MHT is cast in a *probabilistic Bayesian framework*. The ensuing discrete combinatorial optimization problem is solved using a special assignment problem formulation which provides improved efficiency over traditional linear programming (LP) approaches. The *likelihood-based scoring* of data sequences (hypotheses) from this Bayesian formulation allows one to model birth (orbit initiation), survival (orbit continuation), and death (orbit termination) of objects (based, for example, on Poisson processes), probabilities of detection less than one, and one or more frames of data. Additionally, the general framework can accommodate non-Gaussian probability density functions which can be used to more faithfully represent orbit uncertainty needed for both *covariance realism* and *uncertainty realism*. Different methods from non-linear estimation and filtering are also compatible such as the Schmidt-Kalman filter [7], unscented Kalman filter [8], Gaussian sum filters [4, 9], and the Gauss von Mises filter [10, 11]. Moreover, the MHT system supports a specialized *implicit-Runge-Kutta-based orbital propagator* that can propagate multiple orbits simultaneously [12, 13], thereby reducing the computational cost of uncertainty propagation needed in many filtering operations.

The MHT prototype is implemented using modern software practices in a service-oriented and component-oriented architecture, with components implemented in PYTHON and C++. Some low-level algorithms, such as the implicit Runge-Kutta-based orbital propagator [12, 13], are implemented in C++. The MHT components are configured using user-friendly YAML configuration files, and the prototype interacts with the external world via messages. Thus, the system provides the user the ability to plug-and-play different algorithmic components and to evaluate their benefits. An external simulator (or a real data source), data visualization GUIs, metrics dashboards, and metrics computation packages can operate concurrently with the MHT prototype.

In this paper, it is demonstrated that the authors’ prototype MHT system can accurately and efficiently process tens of thousands of UCTs/UCOs emanating from hundreds of closely-spaced objects (and tens of thousands of widely-spaced objects), thereby making it well-suited for large-scale breakup and tracking scenarios. This performance is possible in part due to *complexity reduction* techniques (e.g., gating and orbit hypothesis pruning) that are used to control the runtime of MHT without sacrificing accuracy. Though the authors’ simulations to date have only been run on a single thread of a laptop computer, the scalability of MHT makes it well-suited to high-performance-computing environments.

The focus of this paper is on presenting results on the performance of the MHT prototype. The theoretical framework for MHT was presented in the companion paper [3], together with a description of the component algorithms and software design. The plan of this paper is as follows. Section 2 provides an overview of

---

\*Note, however, that allowing multiple frames of data to arrive and possibly change association decisions does not result in delayed output of established orbits, since the frames are processed in a sliding window and best solutions are reported after every frame is processed.



The term *report* is a generic term used for any input to the MHT, and can be either a UCT or a UCO. The MHT aims to associate (or correlate) the reports to existing objects in the space catalog (i.e., space catalog maintenance). The MHT system can also do joint orbit initiation and UCT/UCO resolution. That is, if the report is not in the space catalog (or if no space catalog is available), the tracker can piece this data together to form high quality orbits (i.e., space catalog generation<sup>¶</sup>). This capability is used, for example, in breakup processing. Thus, MHT performs space catalog maintenance, space catalog generation, and UCT/UCO resolution *jointly*, in a combined system.

**Simulation Framework** In order to validate and test the MHT and its supporting algorithms, an in-house simulation tool was used to generate various scenarios in multiple regimes of space. Scenario generation comprises the following steps:

1. A set of initial conditions for the space objects to be used in the simulation, and a set of sensors, are first chosen by the user. All sensors used in simulation for this paper were ground-based. The user can define various sensor parameters such as their geodetic locations, probabilities of detection, and measurement error standard deviations (sometimes called the “sensor sigmas”). The probabilities of detection for the space objects can also be specified. The probabilities of detection can be less than one.
2. For each space object to be used in a given scenario, its ephemeris is generated over the duration of the scenario using Numerica’s IRK orbital propagator. For objects in LEO, a degree-and-order 32 gravity model is used, and for objects in GEO, a degree-and-order 8 gravity model is used. Ephemerides (DE405) from the Jet Propulsion Laboratory are used for finding the position of the sun and moon. Coordinate frame transformations use the IAU-76/FK5 theory recommended by the International Earth Rotation and Reference Systems Service 1996 Conventions [15].
3. For each sensor-object pair, the time at which the object enters and the time at which the object exits the field of view of the sensor are determined, if applicable, and the average time is recorded. A sensor-object pair revisit schedule scheme and a probability of detection is applied, and if detected, a noisy report is generated at the recorded time. In LEO scenarios, the reports are noisy six-dimensional UCTs represented in equinoctial orbital elements with uncertainties representative, e.g., of a two-minute radar track. Reports for optical sensors are four-dimensional UCOs generated by a quadratic curve fit over a short sequence of measured noisy right-ascension and declination angles [14, 16]. The resulting reports are written to a scenario file. The final scenario file contains all the simulated reports in time order.

**Methodology in LEO (Radar Data)** In scenarios consisting of radar observations of LEO objects, the MHT operates in a UCT-to-UCT association mode, where the input reports to the MHT are all 6-D UCTs (or tracklets) formed from short track segments of range, azimuth, and elevation (RAE) observations. The MHT does not look at the raw RAE measurement sequence of a UCT, and only concerns itself with the estimated tracklet/UCT state and covariances. The task of the MHT in this case is then to partition the “pool” of UCTs into orbits.

For complexity reduction, the MHT makes use of *pair-gating* and *triple-gating* algorithms that use fast methods to rule out several association pairs and triples before forming the tree of all feasible association hypotheses. In LEO, these gates form a hierarchy, where fast orbital element gates are first used to quickly rule out many infeasible associations, and slightly more expensive gates try to cut down the number of remaining feasible associations using fast (e.g., unperturbed Keplerian) dynamical models with proper process noise treatment. As a simple example, consider a case where we begin with one frame<sup>||</sup> containing  $n$  reports, and subsequently receive another frame containing  $n$  reports. The total number of orbit hypotheses in this case would be  $n^2$ . However, instead of performing expensive filtering operations to score *all*  $n^2$  hypotheses,

---

<sup>¶</sup>Space catalog generation is sometimes referred to as *object identification*.

<sup>||</sup>A *frame* is a set of reports such that each report is assigned to at most one object. Typically, the MHT processes reports grouped in such frames, and typically all reports in a frame would be from the same sensor and would be time-proximal. The algorithm for building frames makes use of known sensor and scenario regime characteristics.

cheap gates would first try to rule out a large percentage of these hypotheses. In this way, gating controls the complexity of MHT.

The remaining orbit hypotheses in the tree of all hypotheses within the MHT are scored using an unscented Kalman filter which uses the full force models, and an assignment problem is then solved to determine the best partitioning of the reports into orbits. More details are provided in the companion paper [3].

**Methodology in GEO, MEO, HELO (Optical Data)** In scenarios consisting of electro-optical observations (commonly from objects in GEO, MEO, and HELO), the MHT operates in a more general report-to-report association mode, where a report can be either a 6-D UCT/tracklet or a 4-D UCO. Initially, all reports from optical sensors start out as 4-D UCOs that lack range and range-rate information. However, since a large number of UCOs emanate from GEO or near-GEO objects, a statistical hypothesis test is performed to see if a UCO can be “promoted” to a UCT in GEO (i.e., a test is performed to check if the UCO is consistent with a tight prior hypothesis in GEO). This UCO-to-GEO-UCT promotion test is applied to all UCOs input to the MHT, and any UCOs that cannot be promoted in such a way are hypothesized to emanate from non-GEO regimes and are passed to the MHT as is. For complexity reduction, the MHT makes use of a hierarchy of specialized dynamical gates that operate on UCT-UCT, UCO-UCO, or UCT-UCO pairs. The surviving orbit hypotheses in the tree or all hypotheses are scored using sequential filtering when possible (such as when updating a UCT with another UCT or a UCO) or batch filtering (such as when scoring a sequence of 4-D UCOs without any prior 6-D UCT). Parts of this methodology are discussed in [14] and [17]. Further details are left to a future paper.

**Performance Metrics** Several performance metrics can be defined to assess and verify the performance of the MHT (or any other multi-object tracking system). Note that several of the following metrics use truth information (which is not used in any way during tracker runs, and only used to evaluate the performance after runs have completed). We define the following metrics:

- *Discovered objects (established orbits)* are defined as orbits output by the MHT that meet a certain criteria (e.g., having been updated by a minimum number of reports, and having few misassociations).
- *False positives (misassociations, cross-tags)* are the total number of incorrect associations made to the discovered objects. For a given discovered object, the number of incorrect associations is the total number of reports associated to the object minus the number of reports that do not have the same truth ID as the majority of those associated to the object. (Reports with the same truth ID emanate from the same object.)
- *Correctly associated UCTs/UCOs* are the total number of reports associated to all discovered objects minus the total number of false positives.
- *Unassociated UCTs/UCOs* are the total number of reports in the scenario minus the total number of reports associated to discovered objects.

Several orbit accuracy and filtering metrics (e.g., uncertainty realism) can also be defined and used to evaluate the performance of estimation algorithms. However, for simplicity, we omit the discussion of these more detailed metrics and only present results using the high-level tracking metrics defined above.

### 3. RESULTS IN LEO

This section presents results on the use of MHT for processing radar observations emanating from objects in LEO. Two scenarios are considered. In the first scenario, we demonstrate the MHT’s capability for space catalog maintenance by simulating the entire (unclassified) LEO portion of the space catalog and by processing one day of observations. In the second scenario, we demonstrate the MHT’s capability for breakup processing by simulating and processing a breakup event leading to the creation of up to 512 breakup objects. The scenarios were generated using the approach described in Section 2, details of which will now be given, followed by a discussion of the tracking performance.

**Space Catalog Maintenance Scenario** The current space catalog contains roughly 16,000 active entries. Each day, the JSpOC uses a worldwide network of over 30 space surveillance sensors (radar and optical telescopes) to take 380,000 to 420,000 observations [18]. Assuming that each object in the space catalog has the same likelihood of being observed on a given day, roughly 70% of these observations emanate from objects in LEO (e.g., 11,105 objects were observed between June 18 and July 11, 2013). Since a typical tracklet consists of 5-10 observations, approximately 27,000 to 59,000 tracklets are processed on a daily basis.

In order to demonstrate the MHT’s capability for space catalog maintenance, we simulated a scenario of comparable magnitude to that which is processed daily by the JSpOC (see Table 1). Specifically, 11,105 objects are tracked using 28 SSN radar sensors over a 24-hour period, over which 44,923 tracklets are processed (each object receives an update every 5.9 hours on average). Each object’s drag ballistic coefficient is also estimated together with its 6-D orbital state. The lower-triangular Cholesky factor of the covariance matrix for each tracklet, (in equinoctial orbit elements) is taken to be  $diag(\sigma_a = 5 \text{ km}, \sigma_h = 10^{-3}, \sigma_k = 10^{-3}, \sigma_p = 10^{-3}, \sigma_q = 10^{-3}, \sigma_\ell = 36'')$ , which the authors have found to be representative of a two-minute radar track of RAE measurements. The covariance matrix for each object in the catalog is taken to be  $diag(\sigma_a = 50 \text{ m}, \sigma_h = 10^{-6}, \sigma_k = 10^{-6}, \sigma_p = 10^{-6}, \sigma_q = 10^{-6}, \sigma_\ell = 1.5'')$ , corresponding to that of a high-accuracy orbit.

*Despite the magnitude of this scenario and the fact that it was processed on a single thread of a laptop computer, the MHT (with a 6-frame sliding window) runs in realtime and gives excellent tracking performance (1.2% unassociated tracklets, 100% correctly associated tracklets).* Realtime performance is achieved, in part, because 99.99% of the hypotheses are ruled-out by computationally cheap gating algorithms. For comparison, our implementation of nearest neighbor achieves comparable tracking performance, but requires twice the runtime. This confirms claims made by others regarding tracking performance by single-frame data association methods when used in scenarios consisting of widely-spaced objects [19].

Table 1. Description of the simulated space catalog maintenance scenario.

Orbital Regime	# Objects	# Sensors	# Tracklets	Duration	Update Freq.
LEO	11,105	28	44,923	24 hrs	5.9 hrs

**Satellite Breakup Scenarios** Satellite breakups present a formidable challenge to maintaining persistent SSA because orbits must be established on newly-created, closely-spaced breakup objects before downstream SSA function can begin (e.g., conjunction assessment screening). Owing to the ambiguity of breakup scenarios, establishing such orbits can be difficult; existing single-frame methods (e.g., nearest neighbor) typically require many observations of a given object before its orbit can be established. This delay can be mitigated by the use of multiple-frame methods such as MHT, as will now be demonstrated.

LEO satellite breakup scenarios of increasing difficulty are simulated in the following manner. An object in LEO is selected\*\*, and at the time of the breakup (February 11, 2009),  $N$  objects are created, where  $N = 8, 16, 32, 64, 128, 256, \text{ and } 512$ . Each breakup object starts with the same position as the original object, but has a perturbed velocity. The velocity perturbations are drawn from a normal distribution with a standard deviation of 50 m/s second in each direction (in the inertial frame). The resulting cluster of breakup objects slowly disperses throughout the 33 hour scenario, and observations are simulated from 5 SSN radar sensors (Millstone Hill, Fylingdales, Thule, Ascension, Kwajalein Altair). The lower-triangular Cholesky factor of the covariance matrix (in equinoctial orbit elements) is taken to be  $diag(\sigma_a = 10 \text{ km}, \sigma_h = 10^{-3}, \sigma_k = 10^{-3}, \sigma_p = 10^{-3}, \sigma_q = 10^{-3}, \sigma_\ell = 36'')$ , and is representative of the uncertainty of a low-accuracy orbit belonging to an object that is not in the space catalog (e.g., a UCT).

A description of the scenario is given in Table 2. Objects receive, on average, an update every 1.7 hours. The probability of detection is 0.9, and the number of UCTs ranges from 153 (for the 8-object scenario) to 10,168 (for the 512-object scenario). Ten Monte-Carlo runs are performed for each scenario size, the results of which are averaged. The simulations are run in realtime on a single thread of a laptop computer.

Before conjunction assessment screening and other downstream SSA functions can begin, orbits must be established on the newly created breakup objects. Hence, this metric (established orbits versus scenario

\*\*The initial Keplerian orbital elements are  $a = 7155 \text{ km}, e = 0.001124, i = 74.03^\circ, \Omega = 1.717^\circ, \omega = 90.76^\circ, M = 0.05355$ .

Table 2. Description of simulated breakup scenarios.

Orbital Regime	# Objects	# Sensors	# UCTs	Duration	Update Freq.
LEO	8 – 512	5	153 – 10,168	33 hrs	1.7 hrs

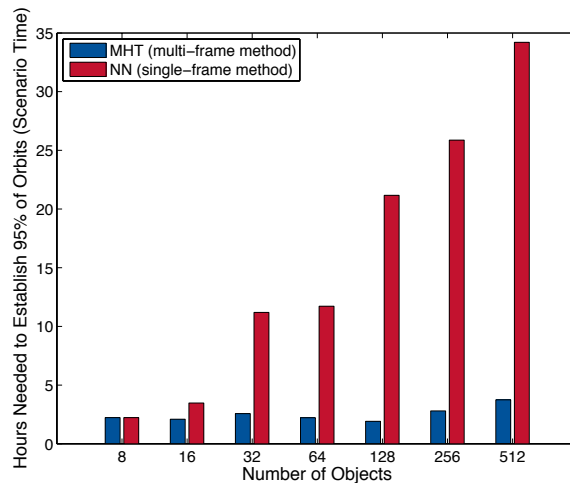


Figure 2. Comparison between MHT and NN regarding the time needed to establish most orbits.

time) provides a high-level quantification of tracking performance. The metric is inferred from the results of running (i) a 6-frame-sliding-window MHT and (ii) a single-frame method, nearest neighbor (NN). Figure 2 demonstrates the scenario time needed to establish 95% of the orbits versus the number of breakup objects. When the breakup is small (8 objects), the time needed to establish 95% of the orbits is nearly the same between MHT and NN. However, as the number of objects increases (as the scenario becomes more difficult), NN requires more and more observations before most orbits can be established, whereas MHT does not. In fact, *MHT establishes most orbits up to 10 times faster than NN* for the large breakup scenarios.

Tracking performance can also be quantified by counting the number of unassociated tracklets/UCTs and the number of correctly associated tracklets/UCTs. This information is summarized in Table 3 for the breakup scenarios. Incorrectly associated tracklets/UCTs (also called cross-tags or false positives) significantly degrade uncertainty realism and make object identification difficult. Unassociated tracklets/UCTs increase computational complexity, may require additional sensor resources, and may result in unnecessary sensor tasking. The results in Table 3 clearly demonstrate the need for more advanced data association methods such as MHT. Note that when calculating the percentage of correctly associated UCTs, unassociated UCTs are excluded. Thus, although 97.4% of UCTs are correctly associated in the nearest neighbor 512-object scenario, 37.7% of the total UCTs could not be associated to any of the established orbits and therefore uncertainty realism will be significantly degraded compared to that of the MHT 512-object scenario.

Table 3. Summary of MHT and NN tracking performance in the simulated breakup scenarios.

Metric	# Objects						
	8	16	32	64	128	256	512
Unassociated UCTs (MHT)	0%	0%	0%	0.1%	0.1%	0.2%	0.3%
Unassociated UCTs (NN)	0%	1.6%	3.1%	5.1%	8.3%	18.3%	37.7%
Correctly Associated UCTs (MHT)	100%	100%	100%	100%	100%	99.9%	99.6%
Correctly Associated UCTs (NN)	100%	99.8%	99.6%	99.5%	98.9%	98.5%	97.4%

#### 4. RESULTS IN GEO, MEO, AND HELO REGIMES

As mentioned earlier, the MHT operates in a substantially different mode to process angles-only reports (UCOs) from EO sensors. To demonstrate this mode, this section presents results on the use of MHT

for processing EO sensor observations emanating from objects in GEO, MEO, and HELO. Three scenarios are considered. In the first scenario, we demonstrate the MHT’s capability for processing reports from 33 closely-spaced objects in the GEO belt representative of GEO clusters. In the second scenario, reports from 220 near-GEO objects, which are more widely spaced than the first GEO scenario, are processed. The maximum eccentricity of objects in the second scenario is 0.01, and the semi-major axes range from 42,150km to 42,180km. The third scenario consists of reports from a mixture of GEO, MEO, and HELO / Molniya objects. In scenario 1, three sensor locations from the GEODSS network were used: Maui, Socorro, and Diego Garcia. For scenarios 2 and 3, measurements representative of nightly sweeps from a single sensor located in New Mexico were simulated. The probabilities of detection range from 0.75 to 0.9. The scenario details are provided in Table 4.

Table 4. Description of the simulated electro-optical sensor scenarios.

Scenario	Orbital Regime	# Objects	# Sensors	# UCOs	Duration	Update Freq.
1	GEO	33	3	2,441	20 days	8 hrs
2	GEO	220	1	14,632	7 days	Nightly
3	GEO, MEO, HELO	821	1	25,989	7 days	Nightly

The results on these scenarios are summarized in Table 5. The metrics used in the table are defined in Section 2. In scenarios 1 and 2, where all objects are GEO or near GEO, the UCO reports are almost always promoted to a 6-D UCT after a statistical hypothesis test is performed to check if the UCOs are consistent with a tight GEO prior, as discussed in Section 2. The performance results show that when a scenario consists of objects mostly in the GEO belt, then the MHT can automatically promote UCOs emanating from these objects to UCT estimates, which results in superior performance both in terms of runtime and association metrics.

Scenario 3 consists of a mixture of objects from the GEO belt and MEO and HELO regimes, and the measurement update rates vary widely amongst the objects. Certain objects remain within the field of view of the optical sensor for longer periods of time than others. This aspect, combined with the fact that many UCOs cannot be promoted to 6-D UCTs, makes this scenario substantially more difficult. Nevertheless, the MHT gives excellent results. We note that in this scenario, the MHT discovers 830 objects, when in fact the true number of objects in the scenario is 821. The fourteen extra objects (also known as “broken” orbits) were established from UCOs/UCTs that should have been associated to other objects. Due to the statistical nature of the estimation algorithms, such broken orbits are always a possibility, and these usually are of short lengths that get dropped after more observations are processed. One of the objective of the MHT is to try to minimize this number. Such broken orbits could be “stitched” together in a post-processing algorithm.

We note that the UCO to UCT promotion algorithm is analogous to the IOD component of constrained admissible region (CAR)-based methods such as CAR-MHF [5]. Therefore, in scenario 1 (where all objects are in GEO) the MHT is able to promote all UCOs to UCTs. Similar results can be obtained using single-frame methods for data association such as nearest-neighbor or the data association component of CAR-MHF. However, in scenarios 2 and 3, UCOs from multiple orbital regimes are encountered. In these scenarios, though CAR-based IOD approaches can be used, they become computationally expensive due to the large number of initial hypotheses (which can be on the order of several hundred for a single object) required to initiate an orbit from a single report. Batch methods, on the other hand, are able to make use of multiple frames of time-diverse data to initiate orbits with a single hypothesis (i.e. with a well-defined range and range-rate)<sup>††</sup>, even in non-GEO regimes.

Table 5 also shows the *gating efficiency*<sup>††</sup> achieved during the runs, and the time (in hours elapsed in scenario time since beginning of scenario) required to establish 95% of the orbits. The actual CPU run time of each scenario is within realtime constraints. For example, scenario 1 spans 20 days but runs in just over 240 seconds on a laptop computer.

<sup>††</sup>The number of sequences over multiple frames to be scored using batch filtering can be substantially reduced using efficient complexity reduction techniques, and need not grow polynomially [2].

<sup>††</sup>The efficiency of a gating algorithm is the total number of pair correlations it declares as infeasible divided by the total number of pairs that represent incorrect correlations. Thus, gating efficiency is a measure of how much complexity reduction a gate achieves.

Table 5. Summary of multi-frame MHT tracking performance in the simulated optical sensor data.

Metric	Scenario 1	Scenario 2	Scenario 3
Discovered objects	33	223	830
Total # of objects in scenario	33	220	821
Correctly associated UCTs	100%	99.97%	99.1%
False positives (misassociations, cross-tags)	0%	0.03%	0.9%
Unassociated UCTs	0%	0%	3.3%
Hours (in scenario time) required to establish 95% of orbits	26.3	6.9	122
Gating efficiency	87.7%	94.6%	79.6%

## 5. CONCLUSIONS

This paper demonstrated the use of a multiple hypothesis tracking (MHT) system for space surveillance in realistic multi-sensor multi-object tracking scenarios in multiple regimes of space. In addition to being fully-automated, the authors' MHT system provides a joint capability for space catalog maintenance, object identification, breakup processing, and UCT/UCO resolution. The results presented in this paper show that the authors' MHT system can process tens of thousands of UCTs/UCOs emanating from hundreds of closely-spaced objects (and tens of thousands of widely-spaced objects) in realtime on a laptop computer. Realtime performance is achieved, in part, due to advanced techniques for complexity reduction, initial orbit determination, and uncertainty propagation. Indeed, good performance of a multiple hypothesis tracking system requires many non-trivial components and a software design that is both flexible and scalable.

In LEO, the MHT system is able to address the challenges of processing breakups by analyzing multiple frames of data simultaneously in order to improve association decisions, reduce cross-tagging, and reduce unassociated UCTs. As a result, the multi-frame MHT system can establish orbits up to ten times faster than single-frame methods. Consequently, downstream SSA functions (e.g., conjunction assessment screening) can begin up to ten times sooner. In GEO, the MHT system is able to address the challenges of processing angles-only optical observations by providing a unified multi-frame framework. In scenarios consisting of reports in GEO, MEO and HELO, the MHT system can detect which UCOs emanate from GEO, and operate in a mode that combines sequential filtering and batch filtering to process scenarios consisting of different types of reports from different types of sensors. Thus, no longer would optical observations need to be thrown out or passed to an external system for (manual) processing. Fewer than 1% of UCTs/UCOs were unassociated in the above scenarios (with the exception of scenario 3 for angles-only data, where 3.3% of UCOs were unassociated). Overall, the results show that the MHT prototype gives excellent tracking performance, in realtime, in large-scale scenarios consisting of reports emanating from objects belonging to different regimes of space.

## ACKNOWLEDGMENTS

The authors thank Sabino Gadaleta for fruitful technical interactions. This work was funded, in part, by a Phase II SBIR from the Air Force Research Laboratory Space Vehicles Directorate (FA9453-11-C-0153), a Phase II SBIR from the Air Force Research Laboratory Information Directorate (FA8750-12-C-0080), and a grant from the Air Force Office of Scientific Research (FA9550-11-1-0248).

## DISTRIBUTION

Approved for public release (Case Number 88ABW-2013-3883).

## REFERENCES

- [1] M. Morton and T. Roberts, "Joint space operations center (JSpOC) mission system (JMS)," in *Proc. of the 2011 AMOS Conference*, (Wailea, HI), Sept. 2011.
- [2] C. A. Sabol, A. Segerman, A. Hoskins, B. Little, P. W. Schumacher Jr., and S. Coffey, "Search and determine integrated environment (SADIE) for space situational awareness," in *Proc. of the 2012 AMOS Conference*, (Wailea, HI), Sept. 2012.

- [3] J. M. Aristoff, J. T. Horwood, N. Singh, and A. B. Poore, "Multiple hypothesis tracking (MHT) for space surveillance: theoretical framework," in *Proc. of the 2013 AAS/AIAA Astrodynamics Specialist Conference*, (Hilton Head, SC), Aug. 2013.
- [4] K. J. DeMars, M. K. Jah, Y. Cheng, and R. H. Bishop, "Methods for splitting Gaussian distributions and applications within the AEGIS filter," in *Proc. of the 22nd AAS/AIAA Space Flight Mechanics Meeting*, (Charleston, SC), Feb. 2012. Paper AAS-12-261.
- [5] K. J. DeMars, M. K. Jah, and P. W. Schumacher, Jr., "The use of short-arc angle and angle rate data for deep-space initial orbit determination and track association," in *Proc. of the Eighth US/Russian Space Surveillance Workshop*, (Wailea, HI), Oct. 2009.
- [6] R. Linares, J. L. Crassidis, M. K. Jah, and H. Kim, "Astrometric and photometric data fusion for resident space object orbit, attitude, and shape determination via multiple-model adaptive estimation," in *Proc. of the 2010 AIAA/AAS Astrodynamics Specialists Conference*, (Toronto, Canada), Aug. 2010. AIAA 2010-8341.
- [7] R. Paffenroth, R. Novoselov, S. Danford, M. Teixeira, S. Chan, and A. Poore, "Mitigation of biases using the Schmidt-Kalman filter," in *SPIE Proceedings: Signal and Data Processing of Small Targets 2007*, vol. 6699, 2007.
- [8] S. J. Julier, J. K. Uhlmann, and H. F. Durant-Whyte, "A new method for the nonlinear transformation of means and covariances in filters and estimators," *IEEE Transactions on Automatic Control*, vol. 55, pp. 477–482, 2000.
- [9] J. T. Horwood, N. D. Aragon, and A. B. Poore, "Gaussian sum filters for space surveillance: theory and simulations," *J. Guidance, Control, and Dynamics*, vol. 34, no. 6, pp. 1839–1851, 2011.
- [10] J. T. Horwood and A. B. Poore, "Orbital state uncertainty realism," in *Proc. of the 2012 AMOS Conference*, (Wailea, HI), Sept. 2012.
- [11] J. T. Horwood and A. B. Poore, "Gauss von Mises distribution for improved uncertainty quantification in space situational awareness," 2013. (To Appear).
- [12] J. M. Aristoff, J. T. Horwood, and A. B. Poore, "Implicit Runge-Kutta methods for uncertainty propagation," in *Proc. of the 2012 AMOS Conference*, (Wailea, HI), Sept. 2012.
- [13] J. M. Aristoff, J. T. Horwood, and A. B. Poore, "Orbit and uncertainty propagation: a comparison of Gauss-Legendre-, Dormand-Prince-, and Chebyshev-Picard-based approaches," *J. Celestial Mechanics and Dynamical Astronomy*, 2013. (To Appear).
- [14] J. T. Horwood, A. B. Poore, and K. T. Alfriend, "Orbit determination and data fusion in GEO," in *Proc. of the 2011 AMOS Conference*, (Wailea, HI), Sept. 2011.
- [15] G. Petit and B. Luzum, "IERS Conventions (2010)," tech. rep., International Earth Rotation and Reference Systems Service, 2010.
- [16] J. M. Maruskin, D. J. Scheeres, and K. T. Alfriend, "Correlation of optical observations of objects in Earth orbit," *J. Guidance, Control, and Dynamics*, vol. 32, no. 1, pp. 194–209, 2009.
- [17] S. M. Gadaleta, J. T. Horwood, and A. B. Poore, "Short arc gating in multiple hypothesis tracking for space surveillance," in *SPIE Proceedings: Signal and Data Processing of Small Targets 2012*, vol. 8393, 2012.
- [18] "USSTRATCOM space control and space surveillance." [http://www.stratcom.mil/factsheets/USSTRATCOM\\_Space\\_Control\\_and\\_Space\\_Surveillance/](http://www.stratcom.mil/factsheets/USSTRATCOM_Space_Control_and_Space_Surveillance/), December 2012.
- [19] K. Hill, C. Sabol, and K. T. Alfriend, "Comparison of covariance-based track association approaches with simulated radar data," in *Proc. of the AAS Kyle T. Alfriend Astrodynamics Symposium*, (Monterey, CA), May 2010. Paper AAS-10-318.